Filensin and Phakinin Form a Novel Type of Beaded Intermediate Filaments and Coassemble De Novo in Cultured Cells

George Goulielmos,* Fotini Gounari,* Susann Remington,* Shirley Müller,§ Markus Häner,§ Ueli Aebi,§ and Spyros D. Georgatos*‡

*Program of Cell Biology, European Molecular Biology Laboratory, 9117 Heidelberg, Federal Republic of Germany; ‡Department of Basic Sciences, Faculty of Medicine, The University of Crete, 711 10 Heraklion, Greece; and §M. E. Müller Institute, Biozentrum, University of Basel, CH 4056 Basel, Switzerland

Abstract. The fiber cells of the eye lens possess a unique cytoskeletal system known as the "beaded-chain filaments" (BFs). BFs consist of filensin and phakinin, two recently characterized intermediate filament (IF) proteins. To examine the organization and the assembly of these heteropolymeric IFs, we have performed a series of in vitro polymerization studies and transfection experiments. Filaments assembled from purified filensin and phakinin exhibit the characteristic 19–21-nm periodicity seen in many types of IFs upon low angle rotary shadowing. However, quantitative mass-per-length (MPL) measurements indicate that filensin/phakinin filaments comprise two distinct and dissociable components: a core filament and a peripheral filament moiety. Consistent with a nonuniform organization, visualization of unfixed and unstained specimens by scanning transmission electron microscopy (STEM) reveals the existence of a central filament which is decorated by regularly spaced 12–15-nm-diam beads. Our data suggest that the filamentous core is composed of phakinin, which exhibits a tendency to self-assemble into filament bundles, whereas the beads contain filensin/phakinin hetero-oligomers. Filensin and phakinin copolymerize and form filamentous structures when expressed transiently in cultured cells. Experiments in IF-free SW13 cells reveal that coassembly of the lens-specific proteins in vivo does not require a preexisting IF system. In epithelial MCF-7 cells de novo forming filaments appear to grow from distinct foci and organize as thick, fibrous laminae which line the plasma membrane and the nuclear envelope. However, filament assembly in CHO and SV40-transformed lens-epithelial cells (both of which are fibroblast-like) yields radial networks which codistribute with the endogenous vimentin IFs. These observations document that the filaments formed by lens-specific IF proteins are structurally distinct from ordinary cytoplasmic IFs. Furthermore, the results suggest that the spatial arrangement of filensin/phakinin filaments in vivo is subject to regulation by host-specific factors. These factors may involve cytoskeletal networks (e.g., vimentin IFs) and/or specific sites associated with the cellular membranes.

INTERMEDIATE filaments (IFs)[1], together with microtubules and actin microfilaments, make up the cytoskeleton of most eukaryotic cells. Their building blocks belong to a superfamily of fibrous proteins which have the inherent tendency to polymerize into 10 nm, ropelike structures. IFs are dynamic entities able to exchange subunits throughout their length. They assemble by lateral and longitudinal growth of small oligomers termed protofilaments. Subfilamentous intermediates of IFs have been identified in a variety of in vitro studies, but the exact arrangement of subunits in the polymer has not been precisely determined (Heins and Aebi, 1994). Biochemical studies and sequence comparisons have established that all IF proteins consist of three structural domains: a central, largely α-helical, "rod" domain and two nonhelical end-regions ("head" and "tail" at the NH_2- and COOH-termini, respectively). The α-helical domain is subdivided into four segments, termed coil 1a, coil 1b, coil 2a, and coil 2b, and has a defined length of either 310 or 352 amino acid residues. Whereas the rod domain contains conserved sequence principles, the end-domains of different IF proteins vary markedly both in length and in sequence. Based on intracellular location, IFs can be distinguished into two broad categories: cytoplasmic IFs and nuclear lamins. The

Address all correspondence to Spyros D. Georgatos, Department of Basic Sciences, The University of Crete School of Medicine, 711 10 Heraklion, Crete, Greece. Tel.: 30 81 542 070 ext. 226. Fax: 30 81 542 112.

1. *Abbreviations used in this paper*: BF, beaded-chain filament; CHO, chinese hamster ovary; IF, intermediate filament; LFC, lens fiber cell; MCF-7, human mammary carcinoma; MPL, mass-per-length; STEM, scanning transmission electron microscopy; SW13, human adrenal carcinoma.

current understanding is that the nuclear lamins, which represent the ancestors of cytoplasmic IFs, are involved in vital functions, whereas cytoplasmic IFs play more subtle, tissue- or cell-specific roles. (For a topical review see Fuchs and Weber, 1994.)

The eye lens represents a simple model system in which structural and functional analyses of IFs can be combined. The cellular and subcellular organization of the lens has been explored in numerous previous studies (for a comprehensive review see Maisel et al., 1981). This organ contains a monolayer of polarized epithelial cells (lens epithelium) which cover its anterior surface. The lens "parenchyma" consists of highly elongated cells, the so-called lens fiber cells (LFCs). The cytoplasm of the LFCs is filled with crystallins, a class of water-soluble proteins believed to minimize scattering of the light that passes through the eye. The LFCs are organized in successive, concentric layers (like an onion) and are tightly connected by a variety of intercellular junctions. Although lacking a cell nucleus, the terminally differentiated LFCs maintain a well-organized spectrin-actin membrane skeleton and possess two different types of IF networks. One network is distributed throughout the cytoplasm and consists of vimentin IFs; the other IF system is located primarily at the cell cortex and comprises heteropolymeric structures composed of filensin (formerly called CP94, CP95, or CP115) and phakinin (formerly called CP49 or CP47). These structures are known as beaded-chain filaments (BFs). Unlike vimentin, which is widely expressed in many cell types, filensin and phakinin are uniquely expressed in the eye lens (for a recent review see Georgatos et al., 1994).

Vimentin IFs do not appear to play a major role in lens function. Knock out of the single vimentin gene in the mouse does not affect lens morphogenesis nor does it change the overall architecture of the LFCs (Colluci-Guyon et al., 1994). From this finding it can be inferred that vimentin IFs are not necessary for normal lens development. However, the reduced synthesis of filensin in a strain of mutant mice (Eye lens obsolescence mouse) has been correlated with severe developmental defects such as the inability of the LFCs to elongate (Masaki et al., 1991).

From a structural viewpoint, the lens-specific IF proteins, filensin and phakinin, represent highly specialized polypeptides, distinct from the other members of the IF family. Filensin shows rather "regional" homology to other IF proteins (mainly in the area of coil 1a and coil 2b) and has a "truncated" rod domain (29–30 amino acid residues in the segment between coil 2a/2b are missing; see Gounari et al., 1993; Remington, 1993). Phakinin has a normal size rod domain, shows extensive sequence similarity to type I keratins, but completely lacks a tail domain (Merdes et al., 1993). Purified filensin self-assembles into short 10-nm-thick fibrils, whereas purified phakinin has been reported to form large aggregates (Merdes et al., 1991, 1993). Although these homopolymeric structures bear no resemblance to ordinary IFs, mixing of purified filensin and phakinin in a 1:3 molar ratio yields normal looking IFs (Merdes et al., 1993).

To investigate the molecular interactions between filensin and phakinin in detail, we performed a systematic in vitro and in vivo study. Data described below shed light on the structural relationships between lens-specific IFs and ordinary IFs and provide clues for the coassembly of filensin and phakinin in vivo.

Materials and Methods

Construction of Bacterial and Eukaryotic Expression Plasmids

A previously isolated 2.5 kb bovine filensin cDNA was ligated into the EcoRI polylinker site of the pT7-7 bacterial expression vector (Studier et al., 1990) and expressed in *E. coli* (BL21). The filensin synthesized from this construct has an NH_2-terminal addition corresponding to the amino acid sequence MARIPARGGA.

A bovine phakinin cDNA (Merdes et al., 1993) was used to prepare suitable constructs encoding full-length phakinin for expression in bacteria. We note here that the previously reported sequence of phakinin (Merdes et al., 1993) contained two sequencing errors which alter the frame in the 5′ region of the cDNA. The corrected sequence has been deposited in the EMBL data bank (file X75160. EMNEW).To generate the phakinin bacterial expression construct, an NdeI site was engineered by amplification with the upstream oligonucleotide GGGAATTCCATATGAGCAC-CAGGCGCGTG in the translation initiation codon of the phakinin cDNA. The resulting fragment was inserted between the NdeI–HindIII sites of the pT7-7 vector.

Eukaryotic expression constructs were generated by subcloning the coding sequences from the corresponding bacterial expression constructs into the PSVK3 vector (Pharmacia, Uppsala, Sweden). Thus, the full-length filensin cDNA was inserted in the PSVK3 as an EcoRI fragment. This construct does not contain the NH_2-terminal additional 10 amino acids present in the bacterial expression construct. An myc tag (Evan et al., 1985) was added to the phakinin eukaryotic expression vector as an NcoI–NdeI insertion, upstream and in frame with the phakinin translation initiation codon. Recombinant DNA manipulations were performed essentially as described in Sambrook et al. (1989).

Bacterial Expression and Purification of Proteins

Logarithmically growing cultures (500 ml, $OD_{600} = 1$) were induced with 0.2 mM isopropyl-β-D-thiogalactopyranoside (IPTG; Biofinex, Praroman, Switzerland). After another 3 h at 37°C, the bacteria were harvested by low-speed centrifugation, the cell pellet resuspended in 1/10 of the original volume in 150 mM NaCl, 10 mM Tris/HCl, pH 7.4, 1 mM PMSF, 2 μg/ml leupeptin, 2 μg/ml pepstatin, 2 μg/ml antipapain and 2 μg/ml aprotinin (lysis buffer), and lysed by sonication at 0°C. The lysates were sedimented at 12,000 *g* for 15 min at 4°C and the pellet was washed with 1% Triton X-100 in lysis buffer. The Triton-insoluble material was washed with 1 M urea and 1% Triton X-100 in lysis buffer. The washed pellet was solubilized in 8 M urea, 10 mM Tris/HCl, pH 7.5, 1 mM EDTA, 1 mM DTT, 2 μg/ml leupeptin, 2 μg/ml pepstatin, 2 μg/ml antipapain and 2 μg/ml aprotinin (urea-Tris extraction buffer), and centrifuged at 12,000 *g* for 45 min at 18°C to remove insoluble material. The clarified urea extract was chromatographed on DEAE-cellulose (DE53, Whatman, Maidstone, GB) using a 1–150 mM NaCl gradient in urea-Tris extraction buffer. Fractions enriched for the protein of interest were pooled and further chromatographed on a hydroxylapatite column (BioRad Labs, Richmond, CA). The column was eluted with a gradient of 10-100 Na_3PO_4 in 7 M urea, 10 mM Na_3PO_4 pH 7.5, 1 mM DTT, 1 mM PMSF (urea-phosphate buffer).

Phakinin was purified either from bacterial lysates (prepared as above), or from fresh bovine lenses obtained from a local slaughterhouse. The lenses were washed three times with ice-cold homogenization buffer (155 mM NaCl, 20 mM Tris/HCl, pH 7.5, 2 mM $MgCl_2$, 0.1 mM EGTA, 1 mM DTT, 1 mM PMSF, 2 μg/ml leupeptin and 2 μg/ml pepstatin) and homogenized in a Waring blender at 4°C. The homogenate was first cleared from debris by spinning at 1,000 rpm for 5 min at 4°C in tabletop centrifuge. After centrifugation for 30 min at 12,000 *g* at 4°C, the pellet was resuspended in 600 mM KCl, 50 mM Tris/HCl, pH 7.5, 2 mM $MgCl_2$, 0.1 mM EGTA, 1 mM PMSF and recentrifuged at 12,000 *g* for 30 min at 4°C. The insoluble material was extracted first with 0.5% Triton X-100 in homogenization buffer and then with low salt buffer (10 mM Tris/HCl, pH 7.5, 1 mM PMSF, 1 mM DTT). The pellet was extracted with 6 M urea, 10 mM Tris/HCl, pH 7.5, 1 mM EGTA, 1 mM DTT and 1 mM PMSF (6 M urea buffer) and centrifuged at 12,000 *g* for 60 min at 18°C. The clarified supernatant was loaded onto a DEAE-cellulose column. Bound material was eluted with a gradient of 0–100 mM KCl in 6 M urea buffer. Phakinin-

enriched fractions were pooled, loaded onto a Superdex-200 gel filtration column (Pharmacia, Uppsala, Sweden) and the column eluted with 6 M urea buffer. Fractions containing purified phakinin were identified by SDS-PAGE in 12.5% polyacrylamide gels.

In Vitro Assembly Experiments

In vitro assembly was performed at protein concentrations of 0.2–0.4 mg/ml, at room temperature. The purified proteins were kept in 6–8 M urea, 10 mM Tris/HCl, pH 7.5, 2 mM EDTA, 1 mM DTT, 2 μg/ml aprotinin, 2 μg/ml antipapain, 2 μg/ml pepstatin, 2 μg/ml leupeptin and 0.5 mM PMSF (urea buffer). To self-assemble phakinin, purified protein was dialyzed from 6 M urea to 160 mM KCl, 20 mM Tris/HCl, pH 7.5, 0.1 mM EGTA, 1 mM $MgCl_2$, 1 mM DTT and 0.5 mM PMSF (isotonic buffer), on ice, for 2–3 h. To self-assemble filensin, the protein was first dialyzed from 8 M urea to 4 M urea for 2 h at room temperature, followed by dialysis against isotonic buffer, overnight at 4°C. Polymerized filensin was pelleted at 400,000 *g* for 40 min at 18°C, solubilized in 6 M urea and dialyzed against isotonic buffer, for 3 h, on ice (recycling). To coassemble filensin with phakinin, the proteins were codialyzed from high urea to decreasing urea concentrations (6–8 M→4 M→2 M→0 M) in isotonic buffer, for 3 h at room temperature.

Electron Microscopy

Samples were prepared for electron microscopy and either negatively stained or glycerol sprayed and low-angle rotary shadowed. To negatively stain in vitro reconstituted polymers, 10-μl aliquots of each specimen were applied to collodium/carbon-coated copper grids. After washing with distilled water, the material was stained with 2% uranyl acetate and air-dried. The grids were then examined in a Phillips 400 or 301 electron microscope. For rotary shadowing, a 20-μl aliquot of each sample was mixed with glycerol to a final concentration of 30% and sprayed onto pieces of freshly cleaved mica. The mica pieces were placed on the table of a high-vacuum evaporation-machine (Balzers BAE 080) for drying and rotary-shadowing with platinum/carbon (using an electron beam source) at an elevation angle of ~3° (Fowler and Aebi, 1983). The mass-per-length (MPL) of phakinin/filensin heteropolymers was determined by quantitative scanning transmission electron microscopy (STEM) of unstained/freeze-dried specimens using a Vacuum Generator (East Grinstead, Great Britain) HB-5 STEM operated at 80 kV, following the procedure described by Engel et al. (1985).

Light Microscopy

Indirect immunofluorescence microscopy was performed as described in Merdes et al. (1991). Specimen preparation for confocal microscopy was essentially the same except that before mounting, ~20 μm "feet" were made on the coverslips. Double immunolabeling was done using various polyclonal anti-filensin antibodies (Gounari et al. 1993), the mAb 9E10 against the myc tag (a gift from S. Fuller, EMBL, Heidelberg, FRG), the mAb 7A3 recognizing vimentin (Papamarkaki et al., 1991), and an anti-keratin 8 mAb (kindly provided by M. Osborn, Max Planck Institute for Biophysical Chemistry, Göttingen, FRG).

Transfection of Cultured Cells

CHO (Chinese hamster ovary) cells were obtained from the Amer. Type Culture Collection (Rockville, MD). MCF-7 human mammary carcinoma cells and SV40-transformed lens epithelial cells were obtained from W.W. Franke (German Cancer Research Center, Division of Cell Biology, Heidelberg, FRG). Clones of SW13 human adrenal carinoma cells were provided by R. Evans (Health Science Center, Denver, CO). Transfections were carried out according to the calcium phosphate precipitation method, essentially as described by Wingler et al. (1979). In short, 10^5 cells were plated onto 6-cm tissue culture plates containing sterile coverslips. The cells were refed on the following day and 4–8 h later 0.5 ml of freshly prepared precipitate containing 10 μg DNA was applied. The precipitate was washed off after 16–20 h and the cells were allowed another 24-h incubation before processing for immunofluorescence microscopy.

Other Methods

SDS-PAGE was performed according to Laemmli (1970). Protein concentrations were measured using a kit (BioRad Labs).

Results

Expression and Purification of Recombinant Proteins

A previously isolated bovine filensin cDNA (Gounari et al., 1993) and a bovine phakinin cDNA (Merdes et al., 1993) were cloned into the bacterial expression vector pT7-7. Recombinant plasmids were used to transform *E. coli* (BL21) cells and the overexpressed proteins extracted from inclusion bodies by 8 M urea and isolated from the urea extracts by chromatographic methods (for details see Materials and Methods). Bovine phakinin was purified from 6 M urea extracts of lens tissue as specified in Materials and Methods. SDS-PAGE profiles of the purified proteins are shown in Fig 1.

Self-Assembly of Filensin and Phakinin

Under isotonic conditions, bacterial filensin formed short fibrils (Fig. 2 *e*) which were similar to the fibrils assembled from native lens filensin (for relevant information see Merdes et al., 1991, 1993). However, the behavior of lens and bacterial phakinin was somewhat different than previously reported. More specifically, previous experiments have shown that lens phakinin self-assembles into metastable filamentous structures, 7–8 nm in diameter, which rapidly aggregate (Merdes et al., 1993). Nevertheless, since the previously used preparations were slightly contaminated with a 40-kD phakinin degradation product (Merdes et al., 1993), we reexamined the assembly process using material purified further by gel filtration (see Mate-

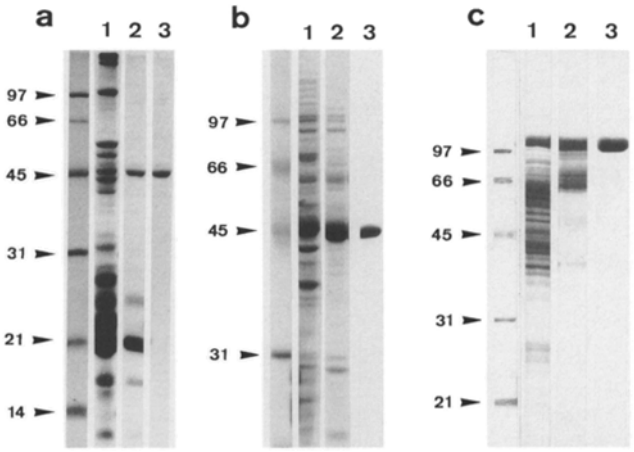

Figure 1. Purification of filensin and phakinin. The figure shows SDS-PAGE stained with Coomassie blue. (*a*) Lane *1*, urea extract of bovine lens-cytoskeleton complexes; lane *2*, phakinin enriched fraction after DEAE-cellulose chromatography (the band at 21 kD probably represents residual crystallins); lane *3*, purified bovine lens phakinin after gel filtration on Superdex 200. (*b*) Lane *1*, urea extract of bacterial inclusion bodies containing recombinant phakinin; lane *2*, phakinin-enriched fraction after fractionation on DEAE-cellulose; lane *3*, purified bacterial phakinin after a second round of chromatography on DEAE-cellulose. (*c*) Lane *1*, urea extract of bacterial inclusion bodies containing recombinant filensin; lane *2*, filensin-enriched fraction after chromatography on DEAE-cellulose; lane *3*, purified bacterial filensin after chromatography on hydroxylapatite. Lanes on the left in *a*, *b*, and *c* represent molecular weight markers with the indicated values (in kD).

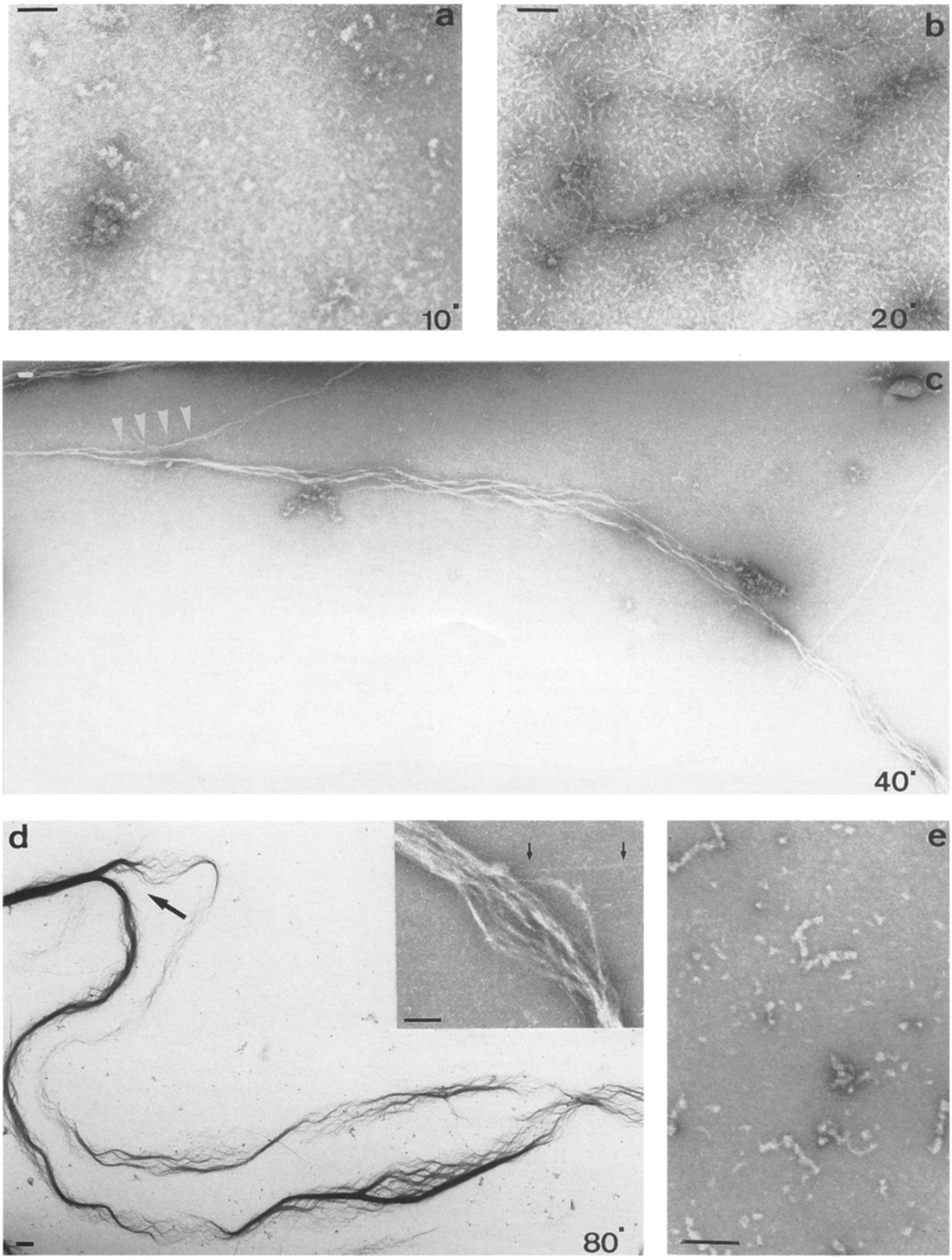

Figure 2. In vitro self-assembly of phakinin and filensin. Purified bovine lens phakinin and recombinant filensin were processed as described in Materials and Methods. Negatively stained samples of phakinin, taken at 10 (*a*), 20 (*b*), 40 (*c*), and 80 min (*d*) after the start of dialysis against isotonic salt buffer are shown in this figure. Arrows and arrowheads indicate subfibers at points where the phakinin bundles unravel. Inset in *d* shows a "bubble" in which the phakinin bundle unravels into protofilamentous strands (*small arrows*). *e* is a negatively stained sample of filensin taken at 90 min after the start of dialysis. Bars represent 100 nm.

rials and Methods) and following a time course approach. As shown in Fig. 2 *a*, gel-filtered lens phakinin dialyzed for very short periods of time (10 min) against isotonic buffer did not form distinct structures. However, at later time points (20 min), we could observe the formation of various fibrillar elements which probably represented protofibrils and higher order oligomers (Fig. 2 *b*). These structures constituted transient intermediates, and, upon further dialysis (40 min), were gradually transformed into filament bundles with an apparent diameter of 50 nm. The phakinin bundles were stable structures and did not aggregate upon further dialysis (80 min). They consisted of helically intertwined filaments which unraveled at points (Fig. 2 *d, inset*). The formation of helical bundles was salt dependent and was not observed when phakinin was reconstituted into low ionic strength media (data not shown). From such observations it would appear that lens phakinin, which is completely tailless, self-assembles into loose, micrometer-long bundles which are much thicker than IFs. Such "thick" filamentous structures are known to form from a variety of tail-truncated or tail-mutagenized IF proteins (for relevant information see Kauffmann et al., 1985; Kouklis et al., 1993; Nakamura et al., 1993; Heins et al., 1993).

In contrast to lens phakinin, bacterial phakinin did not form filament bundles under isotonic conditions, but rather globular particles with diameters of ~100 nm. Although these structures "unfolded" at low salt yielding thick fibrils, they were unable to elongate as much as native lens phakinin filaments (data not shown). The atypical behavior of bacterially produced phakinin was not due to proteolysis or irreversible denaturation, because the *E. coli* expressed protein had the expected molecular weight and was fully competent of copolymerizing with filensin (see below). From this data we infer that self-assembly of phakinin is heavily influenced by posttranslational modifications which do not take place in a prokaryotic environment. Consistent with this interpretation, BF proteins purified from chick lens have been found to be phosphorylated (Ireland and Maisel, 1984).

Ultrastructure and Distribution of Mass in Filensin/Phakinin Copolymers

We have reported previously that lens filensin and phakinin copolymerize in vitro, yielding normal-looking IFs (Merdes et al., 1993). To find out whether the same holds for recombinant proteins expressed in *E. coli*, we codialyzed various filensin and phakinin preparations against isotonic buffer and examined the structures formed by electron microscopy. As shown in Fig. 3, *a* and *b*, lens or bacterial phakinin copolymerized with recombinant filensin into smooth, 10-nm filaments. Slight fixation with glutaraldehyde before staining with uranyl acetate revealed that filensin/phakinin filaments possessed some beadlike structures on their surface (Fig. 3 *d*). To find out whether these beads were an intrinsic feature of the copolymer which was "stripped" by uranyl salts or an artefact due to aldehyde fixation, we proceeded analyzing unfixed specimens by rotary shadowing and scanning transmission electron microscopy (STEM).

Rotary shadowing (Fig. 3 *c*) revealed that in vitro assembled filensin/phakinin filaments exhibit an axial beading with a periodicity of ~19–21 nm, as most other types of IFs (Henderson et al., 1982; Milam and Erickson, 1982; Heins et al., 1993). This characteristic axial periodicity, visible in metal-shadowed but not in negatively-stained preparations, has been previously suggested to represent either the helical pitch of the filaments and/or the periodicity of the protofibrillar coiling, or the approximately half-staggered lateral arrangement of the rod domains of adjacent IF dimers which may be further accentuated by the presence of the end-domains. The filensin/phakinin heteropolymers visualized after rotary shadowing often revealed a spheroidal structure attached at one of their ends (Fig. 3 *c*). Similar observations on filaments that look "tapered" or "annular" have been reported previously (Milam and Erickson, 1982; Henderson et al., 1982; Sauk et al., 1983).

To obtain additional information, we visualized unfixed and unstained specimens by STEM and measured their mass-per-length (MPL) distribution (Engel, 1978). These measurements were done under different conditions. In one setting, filaments assembled from a 3:1 mixture of phakinin and filensin (total protein concentration 250 μg/ml) were diluted 1:2.5 with assembly buffer. Representative histograms are displayed in Fig. 4, *c* and *d* and are indicative of several MPL species for each of the two filament preparations. As illustrated in this figure, we have tried to fit the histograms by multiple Gaussian curves, each of them representing a single MPL species. In more concentrated samples we detected two major MPL peaks at 22 ± 4 and 31 ± 4, and a minor peak at 43 ± 4 kD/nm. However, in less concentrated samples there was only one predominant peak at 19 ± 4 kD/nm. These variations in MPL are within the usual range of variation in ordinary IF preparations (Engel et al., 1985; Troncoso et al., 1989). STEM images of unstained filaments diluted 1:2.5 revealed that the copolymers had a strikingly beaded appearance (Fig. 4 *a*). The beads possessed diameters in the range of 12–15 nm and were distributed in a regular manner along the surface of the filaments with a periodicity of ~19 nm. Some beads with the same dimensions as the beads present on the filaments were also seen in the background (Fig. 4 *a*, *arrowheads*). However, repetition of the in vitro assembly experiments and careful inspection of numerous filaments by STEM indicated that the beading of filensin/phakinin polymers was not always as uniform and as regular as one would expect from stable particles fully integrated into the filament backbone. Thus, it would seem that these structures were peripheral and loosely associated with the filament backbone. Confirming this point, when the preparations were diluted 1:5 with assembly buffer, the filaments appeared no longer beaded and had a definite tendency to unravel into subfilaments (Fig. 4 *b*). The partial unraveling of the filaments was similar to that observed with negatively stained or rotary shadowed preparations of phosphate-treated keratin filaments (Aebi et al., 1983) or with NF-L filaments which often unravel into octameric protofibrils (Aebi et al., 1988). To rule out the possibility that the beads arose from proteolysis of filensin or phakinin in the course of the coassembly, we subjected samples at the beginning and the end of these experiments to SDS-PAGE. No degradation was observed during the assembly experiments (data not shown).

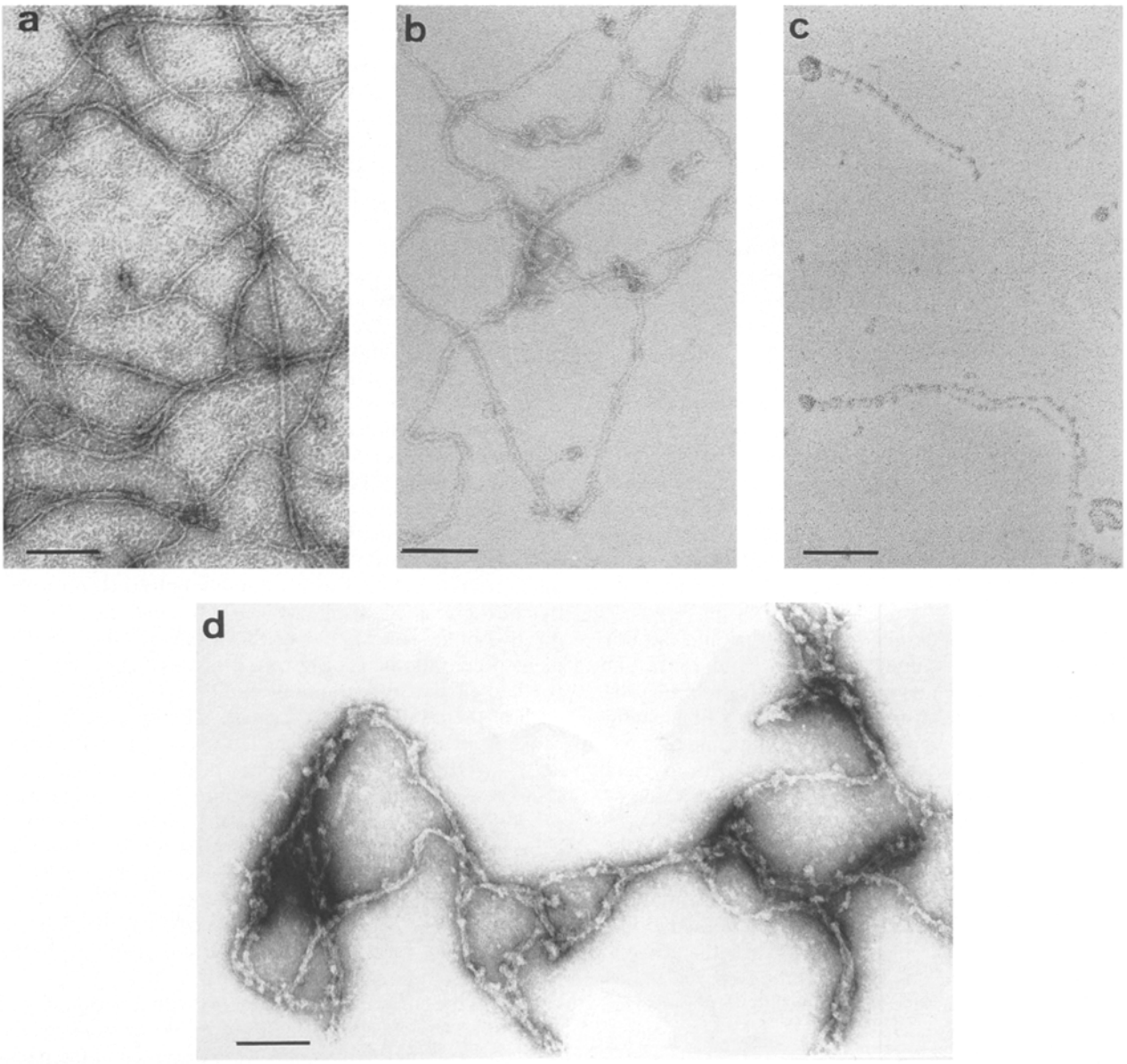

Figure 3. Ultrastructural appearance of filaments assembled from lens or bacterially expressed phakinin and bacterially expressed filensin. (*a*) Bovine lens phakinin coassembled with recombinant filensin and visualized after negative staining. (*b*) Recombinant phakinin coassembled with recombinant filensin and visualized after negative staining. (*c*) Bovine lens phakinin coassembled with recombinant filensin and visualized after glycerol spraying/low-angle rotary metal shadowing. (*d*) Bovine lens phakinin coassembled with recombinant filensin and visualized by negative staining after slight fixation with 0.1% glutaraldehyde. In all of the experiments, the proteins were mixed at a 3:1 molar ratio (phakinin to filensin) and the total protein concentration was 200 μg/ml. For details on the assembly protocol and specimen preparation for EM see Materials and Methods. Bars correspond to 100 nm.

To learn more about the nature of these beads, we determined their mass by STEM. Over 1,000 measurements done in filament preparations diluted 2.5- and 5-fold (see above) yielded one major peak at ~130 kD and three minor peaks at 267, 419, and 617 kD, respectively. These values were very consistent with the mass of a filensin/phakinin heterodimer (M_r = 131 kD) and multimers thereof. Based on the distribution of mass along the native filaments, the mass of the beads, and the ultrastructure of the heteropolymeric filaments we constructed a tentative model representing the substructure of the lens-specific IFs (see Discussion and Fig. 7).

Filensin and Phakinin Coassemble De Novo in Nonlenticular Cells

To examine the coassembly of phakinin and filensin in an in vivo environment, we performed transfection experiments, using the cDNA of filensin and an myc-tagged phakinin cDNA. Tagging of phakinin was necessary because our anti-phakinin antibodies could not detect small amounts of phakinin synthesized in transfected cells. Since LFCs (i.e., the cells which normally express filensin and phakinin) are not maintained in culture, plasmids coding for wild-type filensin or myc/phakinin were transfected indi-

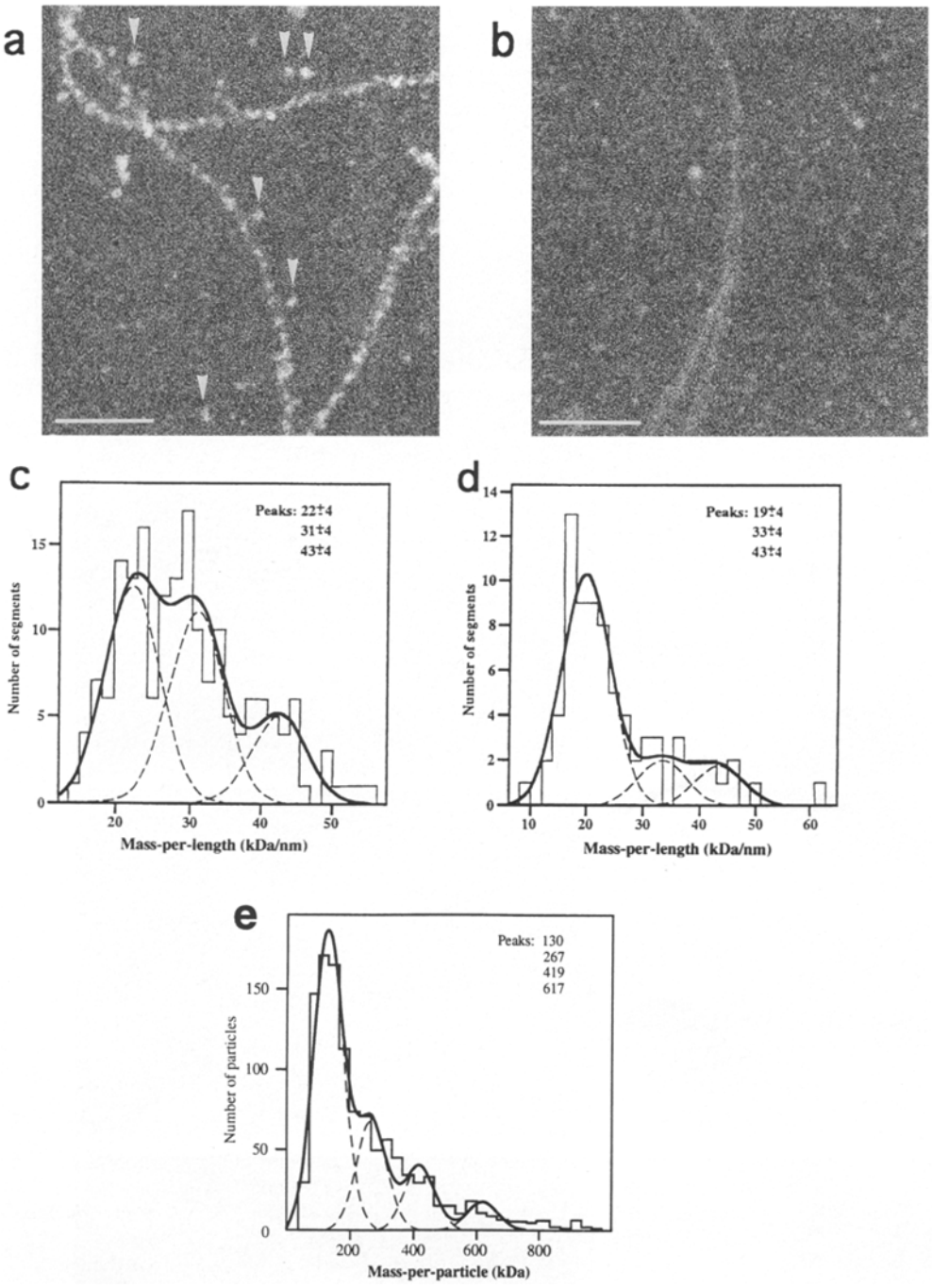

Figure 4. Visualization of unstained/freeze-dried filensin/phakinin filaments by scanning transmission electron microscopy (STEM) and determination of mass per length (MPL) or mass per particle values. (*a*) Appearance of filaments at 100 μg/ml in a sample containing a 1:3 molar ratio of filensin and phakinin. Note the beaded appearance of the filaments and the beadlike particles lying in the background (*arrowheads*). (*b*) Appearance of filaments at 50 μg/ml in a sample containing a 3:1 molar ratio of filensin and phakinin. Note the absence of beads on the filaments and their unraveling into subfilaments. (*c*) MPL values of filaments found in a specimen similar to that shown in *a* (N = 180). (*d*) MPL values of filaments found in a specimen similar to that shown in *b* (N = 77). (*e*) Mass values of beadlike particles found in the background of specimens shown in *a* or *b* (N = 1128). The samples were processed and analyzed as described in Materials and Methods, using an average electron dose of 347 ± 39 e/nm^2 to record the STEM dark-field images. Bars equal 100 nm.

vidually or in combination, into four different cell lines: (*a*) Chinese hamster ovary (CHO) cells, (*b*) SV40-transformed lens epithelial cells (which are fibroblast-like and do not express filensin or phakinin), (*c*) human mammary carcinoma (MCF-7) cells, and (*d*) human adrenal carcinoma (SW13) cells. SV-40 transformed lens epithelial cells and CHO cells express vimentin, whereas MCF-7 cells are known to contain keratins 8, 18, and 19. The clones of SW13 cells used here were free of any of the known types of cytoplasmic IFs (Sarria et al., 1991). All cells were transfected with pSVK3-derived plasmids (see Materials and Methods) and examined 42 h later by indirect immunofluorescence microscopy.

Wild-type filensin or phakinin expressed singly in CHO cells formed aggregates (Fig. 5, *a–d*). Often, the filensin aggregates accumulated near the nuclear envelope and distorted the nucleus (Fig. 5, *c* and *d*). This juxtanuclear localization was never seen upon transfection with phakinin-encoding constructs. In general, the vimentin filament system of CHO cells was not affected by the presence of filensin or phakinin aggregates. However, in most cases, large aggregates containing filensin also contained vimentin, as judged by double immunostaining (data not shown). Coexpression of phakinin and filensin in CHO cells resulted in the formation of heteropolymeric filaments which largely colocalized with vimentin IFs (Fig. 5, *e–h*). Exactly

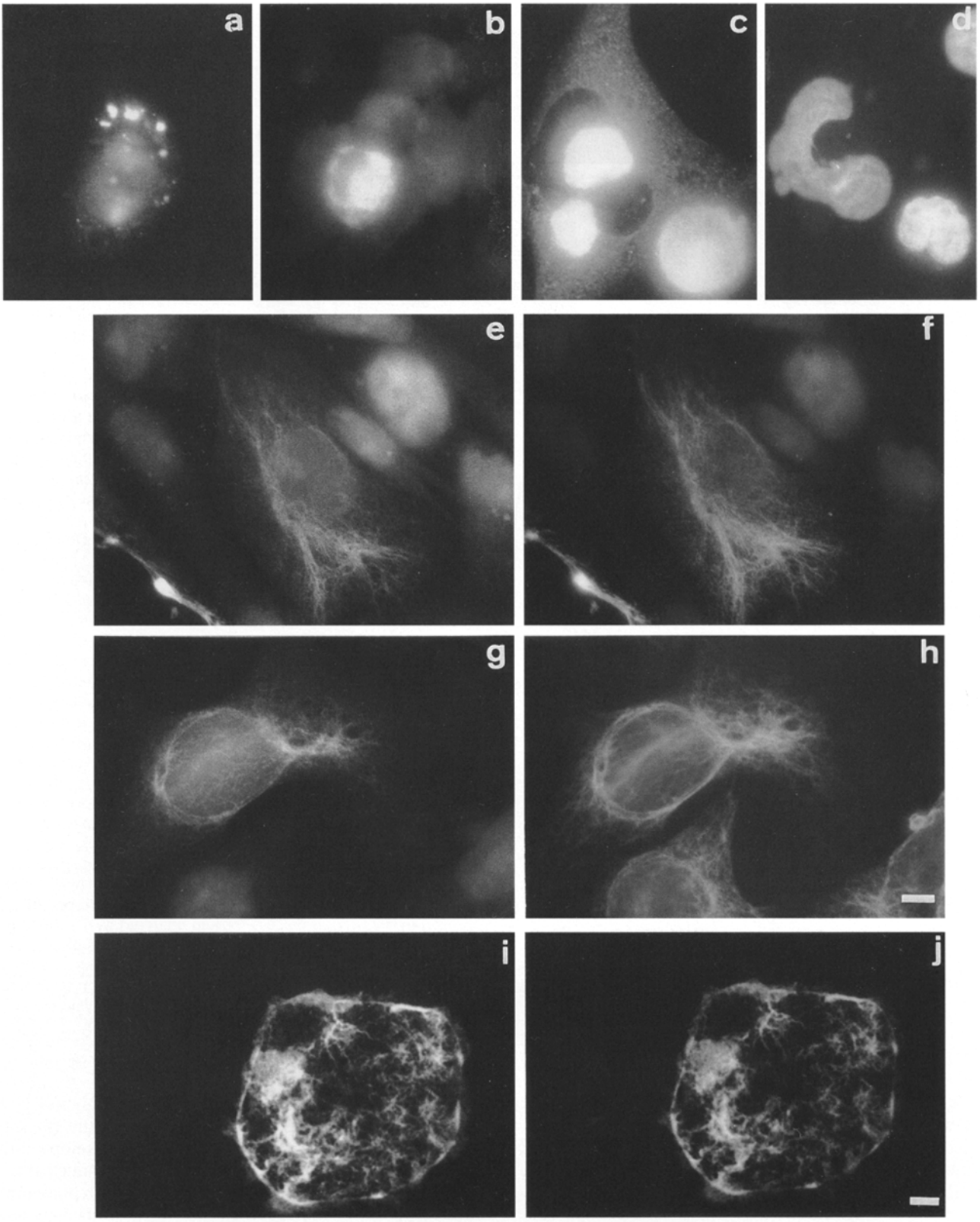

Figure 5. Immunofluorescence staining of transiently transfected CHO and SW13 cells. CHO cells transiently transfected with either myc-tagged phakinin (*a*) or filensin (*b*, *c*, and *d*) expressing plasmids were labeled with the mAb 9E10 against the myc epitope (*a*), or a polyclonal anti-filensin antibody (*b* and *c*). *d* shows DAPI staining of the same field shown in *c* to reveal the deformation of the nucleus by filensin aggregates. CHO cells cotransfected with both plasmids are shown in *e*, *f*, *g*, and *h*. The cells were doubly stained with anti-filensin (*e*) and anti-myc (*f*) antibodies or with anti-filensin (*g*) and anti-vimentin (*h*) antibodies. Notice the colocalization of filensin and phakinin and the codistribution of filensin/phakinin and vimentin filaments. SW13 cells cotransfected with filensin and phakinin doubly stained with anti-filensin and anti-myc antibodies are shown in *i* and *j*, respectively. Bars represent 2 μm.

the same results were obtained when filensin and phakinin were expressed in SV40-transformed lens epithelial cells (data not shown). Of note here is the fact that filamentous networks were observed in ~30% of the cells. Cells which apparently overexpressed filensin or phakinin had a mixed phenotype and contained filaments as well as large spheroidal aggregates. From these experiments we conclude that filensin and phakinin do not form ordered structures when expressed individually, but do coassemble when expressed together. Although we cannot exclude the possibility that the spheroidal aggregates we observed consisted of fibrillar elements, it would appear more likely that self-assembly of filensin and phakinin is inhibited by cellular factors which safeguard IF formation in vivo. A parallel for this has been reported in the case of the NF-L protein (Lee et al., 1993; Ching and Liem, 1993).

To find out whether coassembly of filensin and phakinin requires a preexisting IF network, we also transfected IF-free, SW13 cells. Single transfections yielded a variety of filensin or phakinin aggregates similar to those described above (data not shown). However, cotransfection with constructs coding for the two lens-specific IF proteins yielded filamentous elements primarily distributed in the cytoplasm and occasionally associated with the cell cortex (Fig. 5, *i* and *j*). These filaments were tortuous and anastomosed, but did not appear to be significantly aggregated. Notwithstanding the slightly aberrant features of the heteropolymeric assemblies, we conclude that filensin and phakinin coassemble de novo in IF-deficient cells.

Single transfections of MCF-7 cells with filensin or with phakinin-encoding constructs produced results similar to those described for CHO cells (data not shown). However, when we cotransfected these cells with filensin and phakinin-encoding plasmids, the resultant phenotype was markedly different from that seen in CHO and SW13 cells. In many cases, the newly formed filaments seemed to emerge from distinct foci localized near the plasma membrane or the nuclear envelope (Fig. 6, *a–e*). Filaments emanating from such focal centers often radiated towards the cytoplasm (Fig. 6, *a–d*). However, as more filaments accumulated, parallel arrays of fibers were seen to fold back upon the plasma membrane and the nuclear envelope, forming thick, fibrous laminae. This was particularly evident when specimens were visualized by confocal microscopy (Fig. 6, *g–j*). The submembraneous localization of filensin/phakinin filaments in MCF-7 cells was reminiscent of the distribution of filensin/phakinin filaments underneath the plasma membrane of the LFCs (Merdes et al., 1991, 1993). The de novo formed filaments did not colocalize with the endogenous keratin filaments of MCF-7 cells (Fig. 6, *e* and *f*). Taken together, these observations suggest the existence of factors that can nucleate or anchor de novo assembled filensin/phakinin filaments in MCF-7 cells.

Discussion

Repertoire of Structures Formed by Lens-specific IF Proteins

We have previously suggested that filensin and phakinin constitute obligate heteropolymers (Merdes et al., 1993). Nonetheless, in view of the more detailed studies reported here, it would now seem more appropriate to consider these proteins as facultative heteropolymers. This is because under in vitro conditions, filensin and phakinin self-assemble to a significant extent into non-IF, but yet ordered, structures.

Previously published observations (Merdes et al., 1993) have established that filensin and phakinin are integral components of the lens-specific BFs. However, whereas native BFs have a beaded appearance, in vitro reconstituted copolymers of filensin and phakinin visualized with negative staining do not reveal any obvious beading. To explain this paradox, we have argued that the beads of native BFs may represent either extrinsic components (such as crystallins), or some structural regularities of the filament proper which are not preserved during in vitro assembly and staining with heavy metals (Merdes et al., 1993). In view of the striking images obtained by STEM analysis of unfixed/unstained specimens, and also considering that even negatively stained filaments have a beaded appearance when they are slightly fixed before exposure to uranyl acetate, we now find the second alternative plausible. In support of this interpretation, IFs with a beaded appearance have been observed previously in studies with purified keratins (Sauk et al., 1984), whereas beaded IFs have been identified in the squid giant axon (Eagles et al., 1990). However, it should be noted that the beads detected in filensin/phakinin filaments are labile structures and their perservation seems to depend on physico-chemical parameters that need to be further investigated. This said, the possibility that under in vivo conditions IF-associating proteins bind to periodically repeated sites of filensin/phakinin filaments and further enhance their intrinsic beading is also likely. Recent studies have shown that *a*-crystallins, which are very abundant in the LFCs, bind to various IF proteins and decorate the surface of IFs (FitzGerald and Graham, 1991; Nicholl and Quinlan, 1994).

A Provisional Model for the Packing of Filensin and Phakinin Subunits in BFs

Any model for BF structure should take into account three facts: (*a*) that in vitro assembled filensin/phakinin filaments exhibit a mass-per-length variation from 19 ± 4 kD/nm to 43 ± 4 kD/nm (this study); (*b*) that these heteropolymeric filaments consist of a core filament moiety periodically decorated with beadlike structures (this study); and (*c*) that in vitro assembled filaments as well as native BFs in the LFCs contain approximately three (molar) parts of phakinin and one part of filensin (Merdes et al., 1993). Considering these points, we have constructed a molecular model which incorporates all the available information and describes the packing of subunits in the BFs. This model is schematically depicted in Fig. 7.

We postulate that BFs consist of two, topologically and compositionally distinct filament moieties: (*a*) an inner filament built of eight phakinin homodimers (16 polypeptide chains per filament cross-section which correspond to four protofilaments or two protofibrils); and (*b*) a peripherally disposed filament consisting of eight filensin/phakinin heterodimers (eight filensin and eight phakinin chains per filament cross-section which correspond to four protofila-

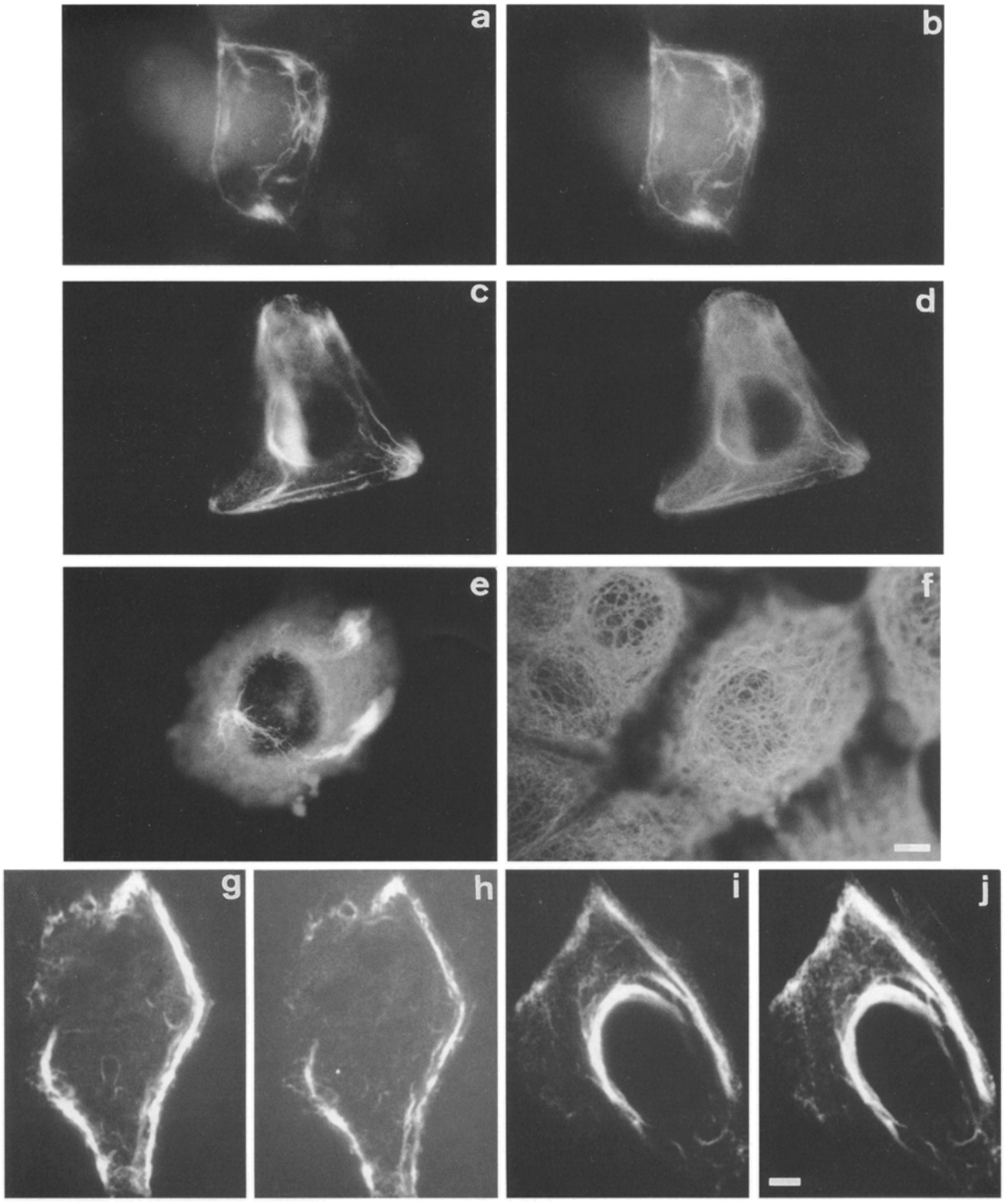

Figure 6. Immunofluorescence staining of transiently transfected MCF-7 cells. Cells cotransfected with plasmids encoding filensin and myc-tagged phakinin were visualized by conventional (*a–f*) or laser scanning confocal (*g–j*) fluorescence microscopy. Samples were doubly stained with anti-filensin (*a*, *c*, *g*, and *i*) and anti-myc (*b*, *d*, *h*, and *j*) antibodies. *e* and *f* show double staining for filensin and keratin 8, respectively. Bars correspond to 2 μm.

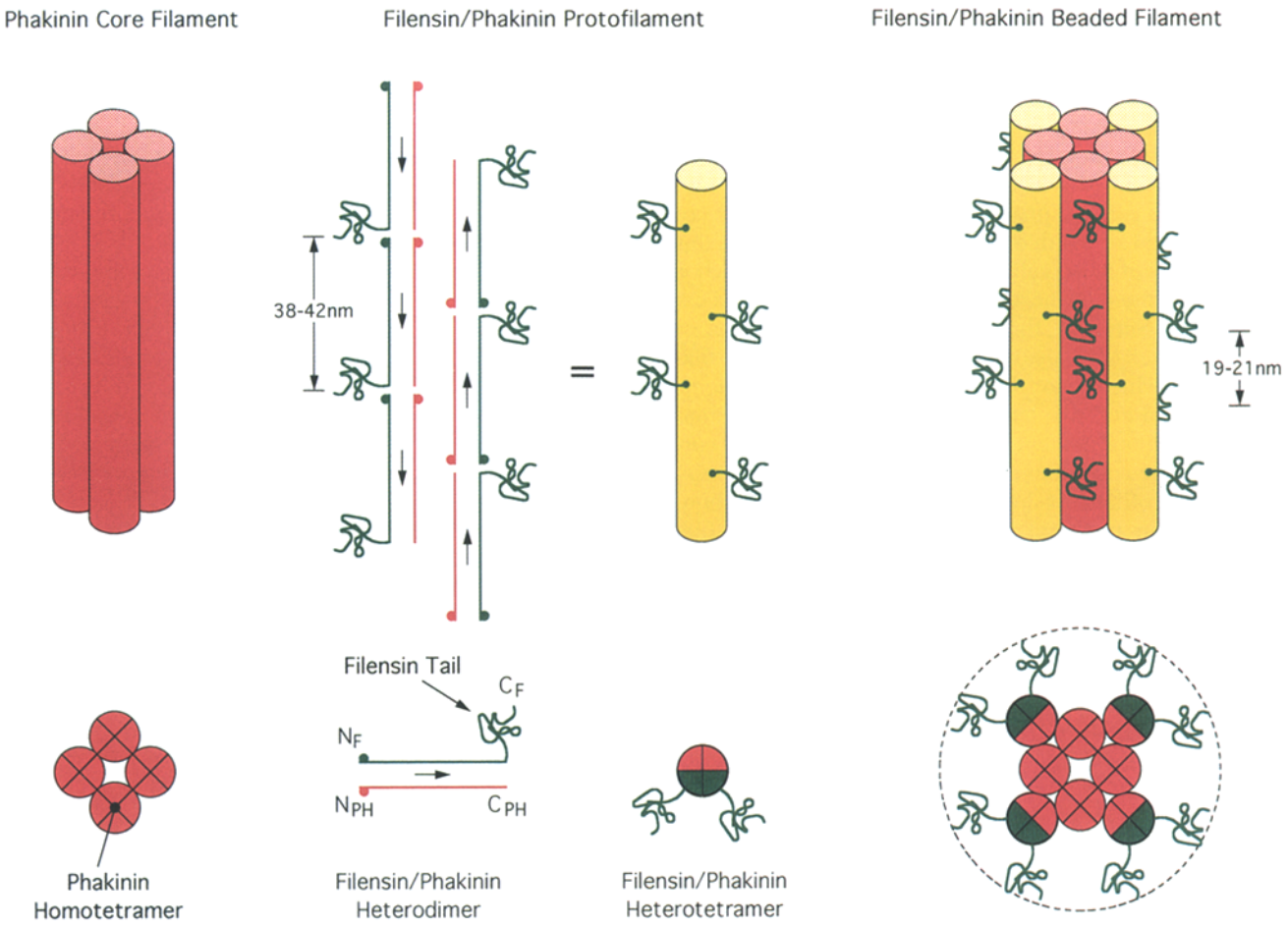

Figure 7. A tentative model for the molecular architecture of heteropolymeric, lens-specific IFs. The filament is depicted as a ropelike structure and is postulated to be built of a core filament moiety composed of four phakinin protofilaments (*red*) and a peripheral filament moiety consisting of four filensin/phakinin protofilaments (*yellow*). The COOH-terminal tail domains of filensin are depicted as convoluted lines (*green*) projecting from the filament core and produce a periodicity of 19–21 nm. Filensin polypeptide chains are shown in green and phakinin chains in red. C_F and N_F are the COOH-terminal tail and the NH_2-terminal head domains of filensin, respectively, while N_{PH} is the NH_2-terminal head domain of phakinin. In an axial projection of a beaded filament, the structure is postulated to contain an inner core (*red*) composed of phakinin and an outer shell composed of filensin and phakinin (*green* and *red*). The beadlike structures depicted in the background of filensin/phakinin filament preparation (see Fig. 4, *a* and *b*) correspond to multiples of filensin/phakinin dimers which detach from the inner core upon dilution of the sample.

mentous strands). Our reasoning is the following: (*1*) examination of unstained filaments by STEM has documented that filensin/phakinin filaments are beaded. The beadlike structures can be dissociated (or partially destroyed) by diluting the sample, leaving behind a core filament which frequently unravels into 2–4 fibrillar strands and has a mass of 19 ± 4 kD/nm. We suspect that this core filament consists of phakinin only because isolated phakinin, unlike filensin, exhibits a tendency to self-assemble into long filamentous structures which comprise loosely connected protofilamentous strands (Fig. 2). These predictions fit very well the mass measurements and the model shown in Fig. 7. Indeed, assuming a molecular mass of 45 kD for phakinin, a repeat length of 38–42 nm (i.e., 2 × 19–21 nm as determined by STEM and rotary shadowing) and an MPL of ~20 kD/nm, we can calculate that the core filament comprises approximately 16.8 polypeptide chains per cross-section, i.e., two protofibrillar or four protofilamentous strands (Number of polypeptide chains per cross-section = Repeat length (r) × MPL/molecular weight [M_r]). (*2*) It is reasonable to assume that the beads on the filaments shown in Fig. 4 *a* represent hetero-oligomers of filensin and phakinin. Indeed, STEM measurements show that the beads which have dissociated from the core filament have masses of 130, 267, 419, and 617 kD, i.e., the mass of a filensin/phakinin heterodimer (131 kD) and multimers thereof. We think that the beadlike morphology of the peripherally disposed filensin/phakinin oligomers should be attributed to the long COOH-terminal domain of filensin which, similar to the COOH-terminal tails of the lamins, may have a compact, globular structure. Since the beads exhibit a periodicity of 19–21 nm, i.e., approximately half the length of the IF rod domain, this would fit an arrangement in which two antiparallel, approximately half-staggered filensin/phakinin heterodimers associate to form a "hybrid" protofilament leaving the COOH-terminal domain of filensin to project out of the filament shaft. (*3*) The 43 ± 4 kD/nm filament species (heavy MPL peak)

identified by STEM most likely represents the fully assembled filament in which each phakinin homodimer in the core filament is connected to a filensin/phakinin heterodimer. Indeed, a beaded filament containing four phakinin protofilaments (4 × 4 × 45 kD = 720 kD) and four filensin/phakinin protofilaments [4 × (2 × 86 kD + 2 × 45 kD) = 1,048 kD] would be expected to have a mass of 1,768 kD and contain phakinin and filensin in a ratio of 3:1. With a repeat length of 38–42 nm (2 × 19–21 nm), this yields a range of MPL values of 42.1–46.5 kD/nm which is in good agreement to the 43 ± 4 kD/nm value obtained experimentally. Similarly, the 32 ± 4 kD/nm filament species ("intermediate" MPL peak) may correspond to a core filament from which two filensin/phakinin protofilaments have detached and two have remained attached, whereas the 19–22-kD/nm filament species ("light" peak) may correspond to the core filament from which all four filensin/phakinin protofilaments have detached. (*4*) Since the bundle of the four phakinin protofilaments in the core filament seems to unravel when the peripherally disposed filensin/phakinin protofilaments are dissociated, it is reasonable to postulate that the latter provide cohesion to the structure of the core filament. The "fasciation" of the core filament by peripheral filensin/phakinin protofilaments may also attenuate the tendency of phakinin to grow laterally into thick bundles.

Overall, the model presented in Fig. 7 shows similarity to the molecular architecture of neurofilaments. Accordingly, neurofilaments are thought to contain an NF-L core and a peripheral shell consisting of NF-L/NF-M and NF-L/NF-H heterotetramers. However, instead of having a globular COOH-terminal tail as with filensin, NF-M and NF-H have extended COOH-terminal tail domains (sidearms) (Hisanaga et al., 1988). Obviously, more information is needed to confirm this tentative model. In the future, biochemical experiments and high resolution morphological studies will address in a more rigorous way the nearest-neighbor relationships between filensin and phakinin subunits in the BF and the mutual arrangement of these building blocks within the core as well as the fully assembled filaments.

Lens-specific IF Proteins Coassemble De Novo in Nonlenticular Cells

Based on the transfection experiments described here, it is clear that wild-type filensin and phakinin coassemble into filamentous structures when expressed together in nonlenticular cells. Thus, the lens microenvironment does not appear to be essential for de novo filament formation. Furthermore, as indicated by transfection of IF-deficient SW13 cells and vimentin-free MCF-7 cells, de novo assembly of heteropolymeric filaments does not require a preexisting IF system. However, since transient expression of filensin and phakinin yields a mixture of phenotypes, we should conclude that the stoichiometry of the two lens-specific polypeptides in each individual cell is a critical determinant of filament assembly.

Although the cellular environment does not seem to affect the ability of lens-specific IF proteins to copolymerize, it clearly affects the distribution of de novo formed filaments. Thus, studies with vimentin-containing CHO cells suggest that filensin/phakinin filaments may interact with vimentin IFs in vivo. Previous in vitro experiments have shown that filensin (but not phakinin) specifically binds to vimentin but does not copolymerize with it (Merdes et al., 1991; Merdes, 1993). Therefore, one is forced to conclude that filensin and vimentin interact at the level of higher order structures rather than forming hetero-oligomers (i.e., dimers, tetramers, or octamers). Future experiments will address this issue in more detail.

At first glance, the colocalization of filensin/phakinin filaments and vimentin IFs in CHO cells appears to be at variance with the spatial arrangement of vimentin and BFs in the LFCs. In lens cells, vimentin filaments and BFs are spatially segregated and seem to associate at a limited number of sites along the cell cortex (Merdes et al., 1991, 1993). One idea that may explain this difference could be that the cellular distribution of BFs is regulated by two opposing factors: (*a*) by their chemical affinity for membrane components (for relevant information see Brunkener and Georgatos, 1992), and (*b*) by their interactions with vimentin IFs or other cytoskeletal elements. The balance between these two interactions may vary depending on cellular context.

The images obtained by analyzing doubly transfected MCF-7 cells provide hints that de novo assembly of heteropolymeric filaments is initiated from a limited number of foci which reside near or at the plasma membrane and the nuclear envelope. Although at this point one does not know whether the filaments physically interact with the membranes, assembly does not seem to occur from random cytoplasmic sites as in the case of vimentin (Sarria et al., 1990). Our results are reminiscent of previous findings where nascent keratin filaments have been reported to assemble in a vectorial fashion when the endogenous IF system was obliterated by incorporation of deleterious, mutant subunits (Albers and Fuchs, 1987). This said, we would like to stress that this point needs further study and does not imply a general mechanism vectorial assembly; instead, the data suggest the existence of alternative pathways of de novo assembly in higher eukaryotic cells (for a review see Georgatos, 1993; Georgatos and Maison, 1996).

This work is dedicated to Stavros and Adamantia Politis. G. Goulielmos was supported by a Human Capital and Mobility fellowship granted by the European Union. S. Remington was supported by a postdoctoral fellowship from the National Science Foundation (USA).

This work was funded in part by a research grant from the Swiss National Science Foundation (31-39691.93) to U. Aebi, the Department of Education of the Kanton Basel-Stadt and the M.E. Müller Foundation of Switzerland.

Received for publication 9 October 1995 and in revised form 13 November 1995.

References

Aebi, U., W.E. Fowler, P. Rew, and T.-T. Sun. 1983. The fibrillar substructure of keratin filaments unraveled. *J. Cell Biol.* 97:1131–1143.

Aebi, U., M. Haner, J. Troncoso, R. Eichner, and A. Engel. 1988. Unifying principles in intermediate filament (IF) structure and assembly. *Protoplasma.* 145:73–81.

Albers, K., and E. Fuchs. 1987. The expression of mutant epidermal keratin cDNAs transfected in simple epithelial and squamous cell carcinoma cells. *J. Cell Biol.* 105:791–806.

Brunkener, M., and S.D. Georgatos. 1992. Membrane-binding properties of filensin, a cytoskeletal protein of the lens fiber cells. *J. Cell Sci.* 103:709–718.

Ching, G.Y., and R.K.H. Liem. 1993. Assembly of type IV neuronal intermedi-

ate filaments in nonneuronal cells in the absence of preexisting cytoplasmic intermediate filaments. *J. Cell Biol.* 122:1323–1336.

Colucci-Guyon, E., M.-M. Portier, I. Dunia, D. Paulin, S. Pournin, and C. Babinet. 1994. Mice lacking vimentin develop and reproduce without an obvious phenotype. *Cell.* 79:679–694.

Eagles, P., H. Pant, and H. Gainer. 1990. Neurofilaments. *In* Cellular and Molecular Biology of Intermediate Filaments. R.D. Goldman et al., editors. Plenum Publishing Corp., New York. pp. 37–94.

Engel, A. 1978. Molecular weight determination by STEM. *Ultramicroscopy.* 3: 273–281.

Engel, A., R. Eichner, and U. Aebi. 1985. Polymorphism of reconstituted human epidermal keratin filaments: determination of their mass-per-length and width by scanning transmission electron microscopy (STEM). *J. Ultrastruct. Res.* 90:323–335.

Evan, G.I., G.K. Lewis, G. Ramsay, and J.M. Bishop. 1985. Isolation of monoclonal antibodies specific for human c-myc proto-oncogene product. *Mol. Cell Biol.* 5:3610–3616.

FitzGerald, P.G., and D. Graham. 1991. Ultrastructural localization of a A-crystallin to the bovine lens fiber cell cytoskeleton. *Curr. Eye Res.* 10:417–436.

Fowler, W., and U. Aebi. 1983. Preparation of single molecules and supramolecular complexes for high-resolution metal shadowing. *J. Ultrastuct. Res.* 83: 319–334.

Fuchs, E., and K. Weber. 1994. Intermediate filaments: structure, dynamics, function, and disease. *Annu. Rev. Biochem.* 63:345–382.

Georgatos, S.D. 1993. Dynamics of intermediate filaments: recent progress and unanswered questions. *FEBS Lett.* 318:101–107.

Georgatos, S.D., and C. Maison. 1996. Integration of intermediate filaments into cellular organelles. *Int. Rev. Cytol.* 164:91–138.

Georgatos, S.D., F. Gounari, and S. Remington. 1994. The beaded intermediate filaments and their potential functions in eye lens. *BioEssays.* 16:413–418.

Gounari, F., A. Merdes, R. Quinlan, J. Hess, P.G. FitzGerald, C.A. Ouzounis, and S.D. Georgatos. 1993. Bovine filensin possesses primary and secondary structure similarity to intermediate filament proteins. *J. Cell Biol.* 121:847–853.

Heins, S., and U. Aebi. 1994. Making heads and tails of intermediate filament assembly, dynamics and networks. *Curr. Opin. Cell Biol.* 6:25–33.

Heins, S., P.C. Wong, S. Muller, K. Godie, D.W. Cleveland, and U. Aebi. 1993. The rod domain of NF-L determines neurofilament architecture, whereas the end domains specify filament assembly and network formation. *J. Cell Biol.* 123:1517–1533.

Henderson, D., N. Geisler, and K. Weber. 1982. A periodic ultrastructure in intermediate filaments. *J. Mol. Biol.* 155:173–176.

Hisanaga, S., and N. Hirokawa. 1988. Structure of the peripheral domains of neurofilaments revealed by low angle rotary shadowing. *J. Mol. Biol.* 202: 297–305.

Ireland, M., and H. Maisel. 1984. Phosphorylation of chick lens proteins. *Curr. Eye Res.* 3:961–968.

Kaufmann, E., K. Weber, and N. Geisler. 1985. Intermediate filament forming ability of desmin and vimentin derivatives lacking either the amino-terminal 67 or the carboxy-terminal 27 residues. *J. Mol. Biol.* 185:733–742.

Kouklis, P.D., M. Hatzfeld, M. Brunkener, K. Weber, and S.D. Georgatos. 1993. In vitro assembly properties of vimentin mutagenized at the β–site tail motif. *J. Cell Sci.* 106:919–928.

Laemmli, U.K. 1970. Cleavage of structural proteins during the assembly of the head of bacteriophage T4. *Nature (Lond.).* 227:680–685.

Lee, M.K., Z. Xu, P.C. Wong, and D.W. Cleveland. 1993. Neurofilaments are obligate heteropolymers in vivo. *J. Cell Biol.* 122:1337–1350.

Maisel, H., C.V. Hardling, J.R. Alcala, J. Kuszak, and R. Brandley. 1981. The morphology of the lens. *In* Molecular and Cellular Biology of the Eye Lens. H. Bloemendal, editor. John Wiley and Sons, New York. pp. 49–84.

Masaki, S., K. Tamai, R. Shoji, and T. Watanabe. 1991. Defect of a fiber cell-specific 94-kDa protein in the lens of inherited microphthalmic mutant mouse Elo. *Biochem. Biophys. Res. Commun.* 179:1175–1180.

Merdes, A. 1993. Filensin und Phakinin: Neue Intermediarfilamentproteine in der Augenlinse. Ph. D. Thesis. University of Heidelberg, Heidelberg, FRG.

Merdes, A., F. Gounari, and S.D. Georgatos. 1993. The 47-kD lens-specific protein phakinin is a tailless intermediate filament protein and an assembly partner of filensin. *J. Cell Biol.* 123:1507–1516.

Merdes, A., M. Brunkener, H. Horstmann, and S.D. Georgatos. 1991. Filensin: a new vimentin-binding, polymerization-competent, and membrane associated protein of the lens fiber cell. *J. Cell Biol.* 115:397–410.

Milam, L., and H.P. Erickson. 1982. Visualization of a 21-nm periodicity in shadowed keratin filaments and neurofilaments. *J. Cell Biol.* 94:592–596.

Nakamura, Y., M. Takeda, S. Aimoto, S. Hariguchi, S. Kitajima, and T. Nishimura. 1993. Acceleration of bovine neurofilament L assembly by deprivation of acidic tail domain. *Eur. J. Biochem.* 212:565–571.

Nicholl, I.D., and R. Quinlan. 1994. Chaperone activity of *a*-crystallins modulates intermediate filament assembly. *EMBO (Eur. Mol. Biol. Organ.) J.* 13: 945–953.

Papamarcaki, T., P. Kouklis, T.E. Kreis, and S.D. Georgatos. 1991. The "Lamin B-fold." *J. Biol. Chem.* 226:21247–21251.

Remington, S.G. 1993. Chicken filensin: a lens fiber cell protein that exhibits sequence similarity to intermediate filament proteins. *J. Cell. Sci.* 103:709–718.

Sambrook, J., E.F. Fritsch, and T. Maniatis. 1989. Molecular Cloning. Cold Spring Harbor Laboratory Press, Cold Spring Harbor, NY.

Sarria, A.J., S.K. Nordeen, and R.M. Evans. 1991. Regulated expression of vimentin cDNA in cells in the presence and absence of a preexisting vimentin filament network. *J. Cell Biol.* 111:553–565.

Sauk, J.J., M. Krumweide, D. Cocking-Johnson, and J.G. White. 1990. Reconstitution of cytokeratin filaments in vitro: further evidence for the role of nonhelical peptides in filament assembly. *J. Cell Biol.* 99:1590–1597.

Studier, F.W., A.H. Rosenberg, J.J. Dunn, and J.W. Dubendorfl. 1990. Use of T4 RNA polymerase to direct expression of cloned genes. *Methods Enzymol.* 185:60–89.

Troncoso, J.C., M. Häner, J.L. March, R. Reichelt, and U. Aebi. 1989. Structure and assembly of specific NF subunit combinations. *In* Springer Series in Biophysics: Cytoskeletal and Extracellular Proteins. U. Aebi and A. Engel, editors. Springer-Verlag, Heidelberg. pp. 33–38.

Wingler, M., R. Sweet, G.K. Sim, B. Wold, A. Pellicer, E. Lacy, T. Maniatis, S. Silverstein, and R. Axel. 1979. T 9 Transformation of mammalian cells with genes from prokaryotes and eukaryotes. *Cell.* 16:777–785.